Molecular Medicine

Xanthohumol Impairs Human Prostate Cancer Cell Growth and Invasion and Diminishes the Incidence and Progression of Advanced Tumors in TRAMP Mice

Roberta Venè,[1] Roberto Benelli,[2] Simona Minghelli,[3] Simonetta Astigiano,[4] Francesca Tosetti,[1] and Nicoletta Ferrari[1]

[1]Molecular Oncology and Angiogenesis and [2]Immunology, IRCCS Azienda Ospedaliera Universitaria San Martino, IST, Istituto Nazionale per la Ricerca sul Cancro, Genova, Italy; [3]Clinical and Experimental Immunology, Istituto Giannina Gaslini , Genova, Italy; and [4]Embryogenesis and Tumorigenesis in Animal Models, IRCCS Azienda Ospedaliera Universitaria San Martino, IST, Istituto Nazionale per la Ricerca sul Cancro, Genova, Italy

Despite recent advances in understanding the biological basis of prostate cancer, management of the disease, especially in the phase resistant to androgen ablation, remains a significant challenge. The long latency and high incidence of prostate carcinogenesis provides the opportunity to intervene with chemoprevention to prevent or eradicate prostate malignancies. In this study, we have used human hormone-resistant prostate cancer cells, DU145 and PC3, as an *in vitro* model to assess the efficacy of xanthohumol (XN) against cell growth, motility and invasion. We observed that treatment of prostate cancer cells with low micromolar doses of XN inhibits proliferation and modulates focal adhesion kinase (FAK) and AKT phosphorylation leading to reduced cell migration and invasion. Oxidative stress by increased production of reactive oxygen species (ROS) was associated with these effects. Transgenic adenocarcinoma of the mouse prostate (TRAMP) transgenic mice were used as an *in vivo* model of prostate adenocarcinoma. Oral gavage of XN, three times per week, beginning at 4 wks of age, induced a decrease in the average weight of the urogenital (UG) tract, delayed advanced tumor progression and inhibited the growth of poorly differentiated prostate carcinoma. The ability of XN to inhibit prostate cancer *in vitro* and *in vivo* suggests that XN may be a novel agent for the management of prostate cancer.

Online address: http://www.molmed.org
doi: 10.2119/molmed.2012.00174

INTRODUCTION

Prostate cancer (PCa) is a serious health concern in Western countries and is the most common cause of death from cancer in men (1). PCa develops and progresses under the influence of androgenic steroids. This influence is consistent with the use of androgen ablation therapies to treat patients with different grades of disease (2). Despite the routine use of diagnostic indicators for PCa development (for example, prostate-specific antigen screening), a high cure rate for localized disease and an increased understanding of PCa biology, most patients will eventually relapse with hormone-refractory PCa, for which available treatment options are only palliative. On the other hand, the fact that PCa onset and progression takes a remarkably long time to occur, and the finding that many premalignant lesions do not progress at all, must be exploited as an important chance for chemopreventive therapies. Effective PCa prevention strategies would spare many men the burden of treatment and could represent the best approach to fight this frequent disease. The molecular biology of PCa and its progression is characterized by aberrant activity of several regulatory pathways within prostate epithelial cells and in the surrounding stromal tissue. One such pathway is the phosphatidylinositol 3-kinase–AKT pathway, which functionally modulates numerous substrates involved in the regulation of cell proliferation/survival, angiogenesis and tissue invasion (3). All these processes represent hallmarks of cancer, and a burgeoning literature is defining the importance of AKT in human and experimental tumorigenesis. In fact, loss of function of phosphatase and tensin homolog deleted on chromosome 10 (PTEN) and AKT activation have been significantly correlated with PCa progression (4).

Active principles in natural products, including plants, are increasingly the subject of intense experimental and clinical research in preventive oncology because of their effectiveness and favorable toxicity profiles (5). Recent studies have shown that xanthohumol (XN), a prenylated chalcone isolated from the hop plant (*Humulus lupulus* L.), inhibits the growth of different types of human cancer cells, including breast, colon, ovaries, prostate and leukemia cells (6–8). XN has been shown to induce both caspase-dependent (9) and -independent (10) apoptosis; to inhibit cell invasion (8), angiogenesis (11) and nuclear factor (NF)-κB activation (11,12); to downregulate topoisomerase I activity and drug efflux transporters expression (13); and to inhibit nitric oxide (14) and prostaglandin E2 production (6). We recently showed that XN targets cell growth, angiogenesis and invasion in acute and chronic myeloid leukemia through AKT/NF-κB inhibition (15,16).

In this study, we investigated the therapeutic potential of XN on PCa cell lines, irrespective of their p53 and PTEN status, and on the onset and progression of PCa in the transgenic adenocarcinoma of the mouse prostate (TRAMP) transgenic mice model. We found a significant activity both *in vitro* and *in vivo*, and we propose that XN might slow the growth of PCa cells via inhibition of the focal adhesion kinase (FAK)/AKT/NF-κB pathways. Our data further support the idea that the AKT/NF-κB inhibitor XN might be a therapeutic option to inhibit the development, progression and metastasis of PCa.

MATERIALS AND METHODS

Cell Culture and Reagent

Androgen-independent DU145 (p53-mutated, PTEN-positive) and PC3 (p53-null, PTEN-negative) prostate carcinoma cell lines (ATCC, Rockville, MD, USA) were cultured in RPMI medium containing 10% fetal calf serum (FCS). DU145 and PC3 subclones adapted to long-term exposure to 10 μmol/L XN (DU145-LTA, PC3-LTA) were established from cultures progressively exposed to increasing concentrations of XN, starting from 1 μmol/L and cloning by limiting dilution. Surviving cells were periodically grown in regular medium to recover and were immediately frozen. In the presence of 10 μmol/L XN, cell lifespan did not exceed 1 month, indicating that both DU145 and PC3 cells were unable to completely evade XN activity. XN and *N*-acetyl-L-cysteine (NAC) were from Sigma-Aldrich (Milan, Italy), dichlorofluorescein diacetate (H$_2$DCFDA) was from Life Technologies (Monza, Italy), and insulin growth factor (IGF)-I and tumor necrosis factor (TNF)-α were from Peprotech (Rocky Hill, NJ, USA).

Cell Proliferation, Migration and Invasion Assays

In vitro cell proliferation was tested on cells plated in 96-well plates at 3,000 cells/well density in complete medium and treated as described. The medium was changed every 2 d. At different time points, the number of viable cells was evaluated by the crystal violet assay.

To perform cell cycle analysis, 0.5×10^6 cells exposed 72–96 h to XN or left untreated were collected, fixed in 1 mL ice-cold 70% ethanol (1 h at 4°C) and permeabilized with 100 μL 1% Triton (1 h at 4°C). Cells were then washed in phosphate-buffered saline (PBS) and incubated in the dark with 50 μg/mL propidium iodide for 30 min at room temperature. After washing, samples were resuspended in PBS and immediately analyzed by flow cytometry (CyAn; Beckman Coulter, Milan, Italy). DNA histograms were created by using the MODFIT LT 3.2 software (Verity Software, Topsham, ME, USA).

Apoptosis was assessed by flow cytometry by using the annexin V–fluorescein isothiocyanate (FITC)/propidium iodide (PI) apoptosis detection kit (Bender MedSystems, Vienna, Austria) following the manufacturer's instruction. Western blot analysis of caspase 3 and poly (ADP-ribose) polymerase 1 (PARP-1) on cell lysates was also performed (rabbit polyclonal antibodies; Cell Signaling Technology, Beverly, MA, USA).

Chemotaxis and chemoinvasion assays were carried out in Boyden chambers as previously described (17). The cells (12 × 10^4/chamber) were extensively washed with PBS, resuspended in serum-free media (SFM) and placed in the upper compartment with or without XN. The two compartments of the Boyden chamber were separated by 8 μm pore-size polycarbonate filters coated with 5 μg/50 μL/filter of collagen type IV for the chemotaxis assay, or with Matrigel (60 μg/filter) for the invasion assay. Serum-free 24 h–conditioned medium from human fibroblasts (FB-CM) was used as a chemoattractant in the lower compartment. After 5 h of incubation at 37°C in 5% CO$_2$, the filters were recovered, fixed in ethanol and stained with Toluidine blue after removal of the non-migrating cells on the upper surface. The migrated cells were quantified by counting five to ten fields for each filter under a microscope. Graphical results are shown as percent inhibition compared with a 100% untreated control. In parallel experiments, trypan blue exclusion under all the conditions tested showed no altered viability compared with controls during the 5 h of the test.

Scratch wound healing assay was carried out on cells grown to 90% confluence in six-well plates and left for 24 h in SFM to block cell proliferation. Wounds were created by scratching cells with a sterile 200-μL pipette tip, with the adherent monolayer washed twice with PBS to remove floating cells and then incubated in RPMI 5% FCS in the absence or presence of XN for 16–24 h. Cell migration was monitored by visual inspection under an inverted microscope and imaging of fixed wound surface fields at various time points. The 4′,6-diamidino-2-phenylindole (DAPI) nuclear counterstain was performed to exclude different proliferation rate of cells at the margin of scratches.

Detection of Intracellular Reactive Oxygen Species

PCa cells (10^5/well) were treated with 10 μmol/L XN for different lengths of time in the absence or presence of the an-

tioxidant NAC at 10 mmol/L. Thirty minutes before the end of the treatment, the cells were incubated with 5 μmol/L H₂DCFDA for reactive oxygen species (ROS) detection. The cells were then washed twice with phenol-free Hanks balanced salt solution, and fluorescence intensity was analyzed with a microplate fluorometer (Molecular Devices, Sunnyvale, CA, USA) with excitation set at 488 nm and emission at 530 nm.

Protein Extraction, Western Blot and Enzyme-Linked Immunosorbent Assay Analyses

Proteins were obtained from PCa cells after a 5-h culture in SFM in the absence or presence of XN and NAC as described in the text and figures. To evaluate AKT activation, cells were serum-starved for 16 h and then treated as indicated; 30 min before the end of the incubation, the cells were stimulated with IGF-I (100 ng/mL). The cells were then lysed in RIPA buffer containing protease inhibitors. To test for NF-κB activation, cells were serum-starved for 16 h and then treated with 5 μmol/L XN for 5 h in SFM in the absence or presence of 10 mmol/L NAC. Thirty minutes before the end of incubation, cells were stimulated with TNF-α (10 ng/mL). Nuclear and cytoplasmic protein extracts were prepared with the nuclear/cytosol fractionation kit (MBL, Woburn, MA, USA) following the manufacturer's instructions. Protein concentration was determined with the DC Protein Assay Kit (Bio-Rad, Segrate, Italy). Equal amounts of proteins were resolved by sodium dodecyl sulfate–polyacrylamide gel electrophoresis (SDS-PAGE), transferred to nitrocellulose and probed at 4°C overnight with the following anti-human antibodies (Cell Signaling Technology): rabbit polyclonal anti-phospho-FAK(Tyr397), FAK, phospho-AKT-1 (Ser473), AKT and phospho-p65 (Ser539). After washing, the blots were incubated for 1 h at room temperature with horseradish peroxidase–conjugated secondary antibodies (Cell Signaling Technology) followed by enhanced chemiluminescence (GE Healthcare, Milan, Italy). An
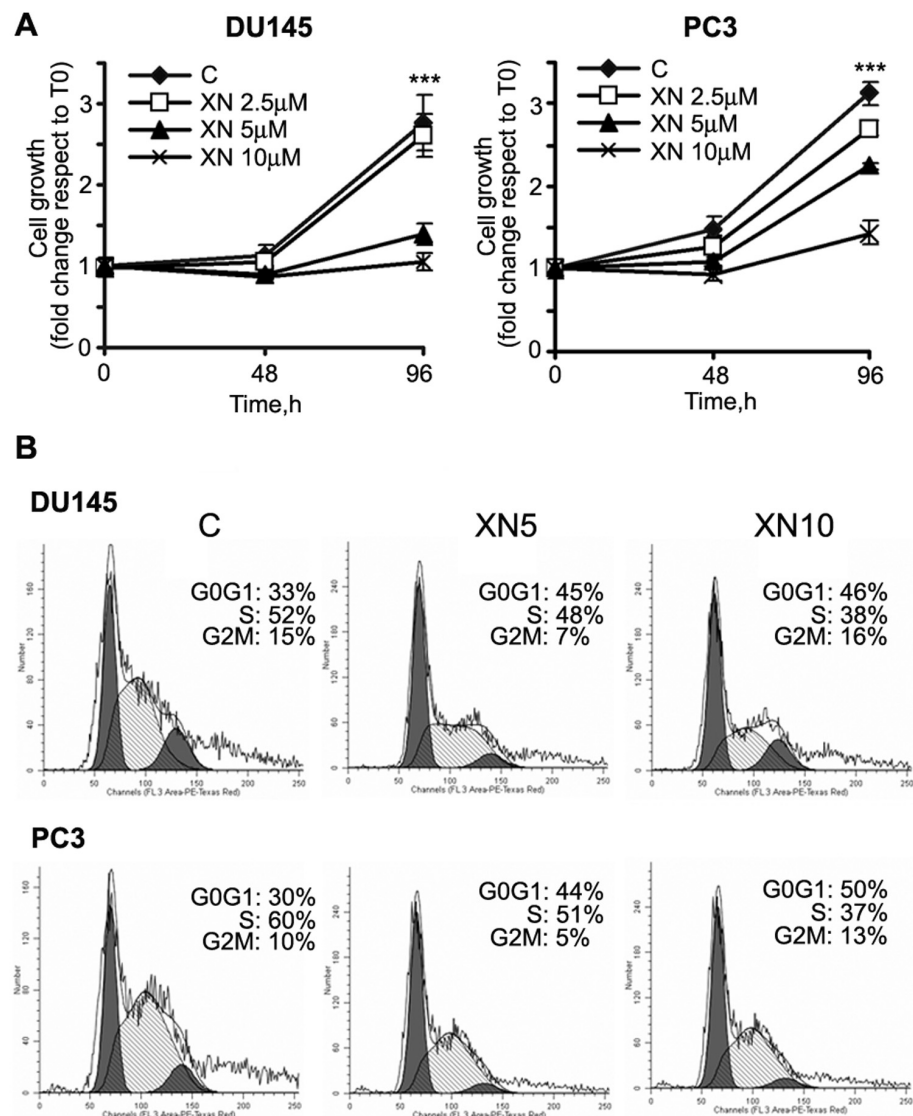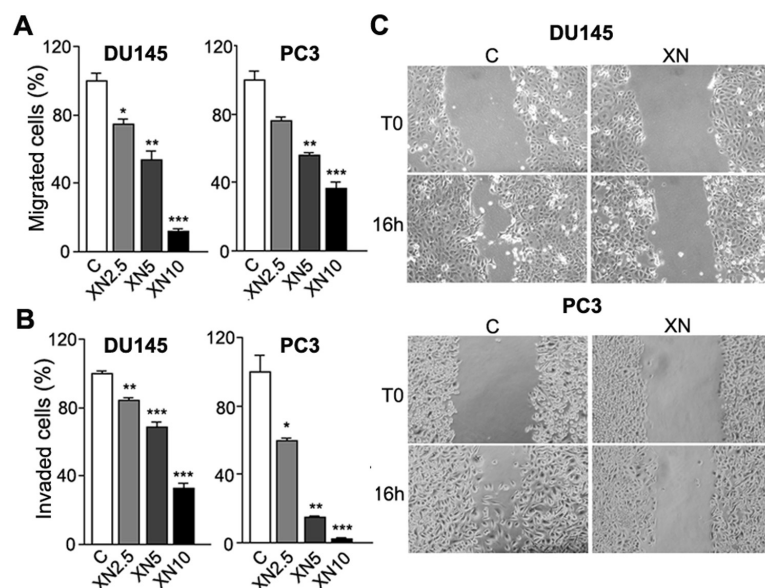

Figure 1. XN treatment inhibits PCa cell proliferation with accumulation in G0/G1 phase. (A) Cell proliferation, evaluated by the crystal violet assay, is significantly inhibited by 5 and 10 μmol/L XN after 96 h exposure (***P < 0.001). Samples were analyzed in sextuplicates (means ± standard deviation (SD) are shown), and each experiment was repeated thrice. (B) DU145 and PC3 cells were treated with XN (5–10 μmol/L) for 72 h and stained with propidium iodide. DNA content was analyzed by flow cytometry. Results are expressed as percent of cell population in G0/G1, G2/M and S phases of the cell cycle. The experiment was repeated two times, and representative data are shown. C, control.

anti-GAPDH antibody conjugated to horseradish peroxidase (Novus Biologicals, Milan, Italy) or a mouse monoclonal anti-β-tubulin antibody (Sigma-Aldrich) were used as loading controls.

NF-κB activity was further analyzed using a commercially available enzyme-linked immunoassay (ELISA) kit

(TransAM; Active Motif, La Hulpe, Belgium) following the manufacturer's instructions. Vascular endothelial growth factor (VEGF) released into the media by PCa cells was measured using a commercial human ELISA kit (BioSource, Invitrogen; Life Technologies, Carlsbad, CA, USA).

Figure 2. XN treatment inhibits PCa cell migration and invasion. Migration (A) and invasion (B) assays were performed in Boyden chambers with conditioned media from human fibroblasts, since chemoattractants reveal a significant reduction of migratory and invasive capacity of XN-treated DU145 and PC3 cells. Experiments were done in triplicate and repeated thrice. Means ± SD are shown (*$P < 0.05$, **$P < 0.01$, ***$P < 0.001$). Migration inhibition by XN was detected by the wound-healing assay (C): monolayers of DU145 and PC3 cells were scraped and treated with 10 μmol/L XN. Cell migration was evaluated by photographing the same fields of the wound surface under an inverted microscope (10× magnification) at time 0 and after 16 h. Representative results from one of three independent experiments are shown. C (within all panels), control; T0, time zero.

Animals and XN Treatment

Use of TRAMP C57BL/6 mice for the studies described herein was approved by the Institutional Animal Care and Use Committee and complied with the *Guide for the Care and Use of Laboratory Animals* (18). Animals were maintained in heterozygosity, and transgene verification was carried out by using DNA obtained from tail clippings as described by Greenberg *et al.* (19). XN was suspended in ethanol (2.5 mg/mL) and further diluted for appropriate concentration. XN (50 μg/mouse) or vehicle alone were administered every other day by gavage in 0.2 mL of 1% polyvinylpyrrolidone and 0.01% Tween 20 to TRAMP mice (10 animals/group, two experiments) beginning at 4 wks and continuing until the animals were 24 wks old, at which time the experiment was terminated. During the experiment, mice were fed food and water *ad libitum*, and body weight was recorded

once every week. Mice were sacrificed by CO_2 inhalation; the urogenital (UG) apparatus consisting of the bladder, urethra, seminal vesicles and the prostate was excised, removed and weighed. The prostate gland was then isolated and a half of the prostate/tumor tissue encompassing the dorsal, ventral and lateral gland was fixed overnight at 4°C in 4% paraformaldehyde, dehydrated in ethanol and paraffin-embedded for histology and immunohistochemical analysis.

Pathologic Evaluation and Immunohistochemical Analysis

Consecutive serial sections (3 μm) were cut at different levels for each sample of paraffin-embedded tissues and mounted on slides. The sections were stained with hematoxylin and eosin (H&E) and evaluated for the presence/absence of the following lesions: prostatic intraepithelial neoplasia (PIN: low,

high), well-differentiated (WD) adenocarcinoma, poorly differentiated (PD) adenocarcinoma with a neuroendocrine phenotype (as demonstrated by synaptophysin staining [data not shown]) and Phylloides-like (PHY) lesions as described (19,20). Randomly selected fields on several H&E-stained sections of individual mice from control and XN-treated groups (10 animals/group: total 100 fields/group) were independently blind-scored by three investigators.

PD adenocarcinomas in TRAMP mice were characterized by a massive vascularization, with large vessels filling the entire tumor mass. We evaluated the status of these vessels by analyzing 10-μm-thick tissue slices without chemical or immunological counterstaining, as described (21). Thick slices of tissue show vessel walls filled with erythrocytes, characterized by strong pale-yellow autofluorescence, when analyzed under a fluorescence microscope with a triple-band filter. Microscope images of control and XN-treated tumors were taken to document the leakiness of vessels in terms of vascular diameter and erythrocyte extravasation.

Statistical Analysis

Experimental data were statistically analyzed by an unpaired two-tailed *t* test, a one-way analysis of variance test followed by a Bonferroni posttest using GraphPad Prism Software and a Fisher exact probability test. *P* values <0.05 were considered significant (*$P < 0.05$, **$P < 0.01$, ***$P < 0.001$).

All supplementary materials are available online at www.molmed.org.

RESULTS

Low-Dose XN Decreases Cell Proliferation in Androgen-Independent PCa Cell Lines

The growth inhibitory and apoptotic effects of high-dose XN in various PCa cell lines has been reported (12,22). While aiming at setting up an experimental model of long-lasting/chronic interventions for primary prevention in high-risk
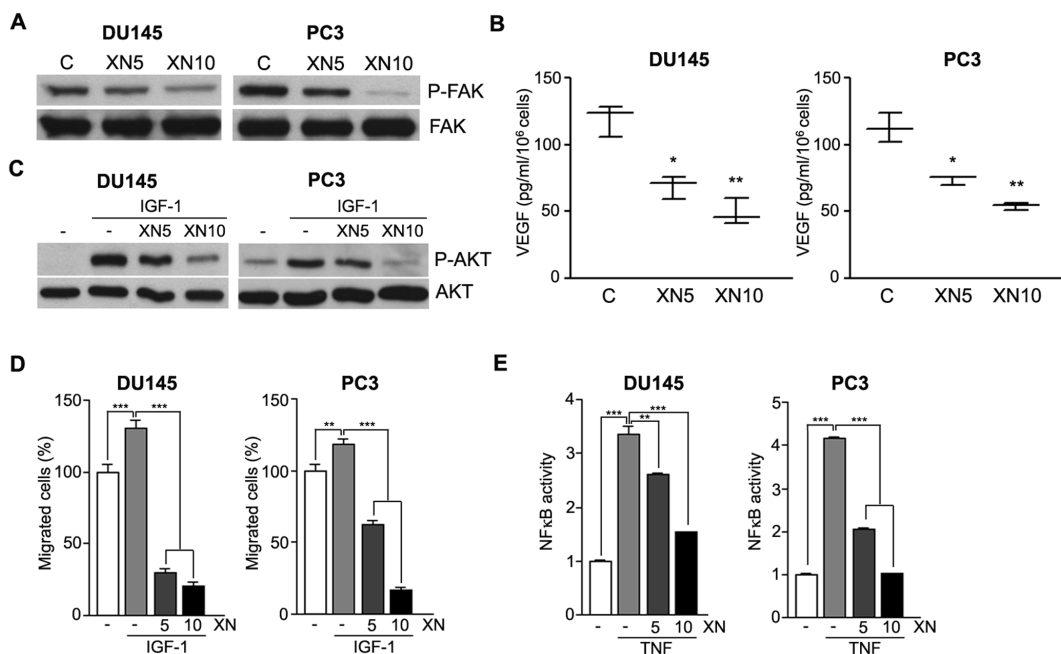
Figure 3. XN inhibits FAK, AKT and NF-κB activation and controls VEGF release and the migratory potential of PCa cells. Western blot analyses show a remarkable decrease of constitutive FAK phosphorylation after 5 h of treatment with XN (A), which correlates with reduced VEGF secretion by DU145 and PC3 cells exposed for 16 h to the drug and analyzed by ELISA (B). Means ± SD are shown (*$P < 0.05$, **$P < 0.01$). (C) Western blot analyses of lysates from DU145 and PC3 cells pulsed for 30 min with IGF-I at 100 ng/mL show a strong induction of AKT phosphorylation, almost completely abolished by 5-h pretreatment with 10 μmol/L XN. Representative results from three independent Western blot experiments are shown. (D) DU145 and PC3 cell migration is significantly enhanced by IGF-I (100 ng/mL), compared with control cells. IGF-I effect is completely abrogated when cell migration is carried out in the presence of XN (5–10 μmol/L). Experiments were done in triplicate and repeated thrice. Means ± SD are shown (***$P < 0.001$). (E) ELISA analyses show that 5 h treatment with XN (5–10 μmol/L) reduces the amount of active NF-κB in TNF-α (10 ng/mL) DU145- and PC3-stimulated cells. Means ± SD are shown (**$P < 0.01$, ***$P < 0.001$). C (within panels A and B), control.

subjects or secondary prevention in cancer patients, the experiments were carried out in the presence of low XN concentrations (2.5–10 μmol/L). We first assessed cell proliferation in PCa cell lines. A total of 5 and 10 μmol/L XN significantly inhibited cell growth (Figure 1A) after 96 h. XN showed an IC_{50} (inhibitory concentration 50) of 6.9 and 9.8 μmol/L at 96 h in DU145 and PC3 cells, respectively. Under these culture conditions, apoptosis was almost absent at 24 and 48 h, as demonstrated by annexin V–FITC binding, lack of caspase 3 and 7 activation and PARP-1 cleavage (data not shown). A small percentage of apoptotic cells could be detected only after 96 h exposure (Supplementary Figure S1), as previously described (22).

Flow cytometry analysis of cell cycle distribution indicated that inhibition of PCa cell growth by XN was mainly due to accumulation in the G0/G1 phase and concomitant reduction in the percentage of cells in the S phase. As shown in Figure 1B, 33% of control DU145 cells were in the G0/G1 phase of the cell cycle, whereas, after treatment with XN (5 and 10 μmol/L) for 72 h, the percentage increased to 45 and 46%, respectively. Similarly, in PC3 cells, G0/G1 cells increased from 30% in control cells to 44 and 50% in cells exposed to 5 and 10 μmol/L XN, respectively.

XN Decreases Cell Migration and Invasion

Migration of cancer cells is one of the key factors responsible for cancer metastasis. The effects of XN on PCa cell migration and invasion were then tested in a dose-response experiment. Untreated PCa cells migrated (Figure 2A) and invaded through Matrigel (Figure 2B) in response to fibroblast conditioned medium (FB-CM). A very short exposure (5 h) to micromolar concentrations of XN significantly inhibited migration (see Figure 2A) and invasion (see Figure 2B) of DU145 and PC3 cells. To further examine the inhibitory effect of XN on PCa cells motility, the scratch wound healing assay was performed. After 16- to 24-h incubation, control cells migrated into the scratch wound, whereas the wound closure area was almost free of cells in cultures treated with 5 or 10 μmol/L XN. The results confirmed that XN could inhibit the migration of PCa cells (Figure 2C; 16-h exposure to 10 μmol/L XN is shown). DAPI nuclear counterstain revealed similar levels of mitosis in control and treated cells, suggesting that
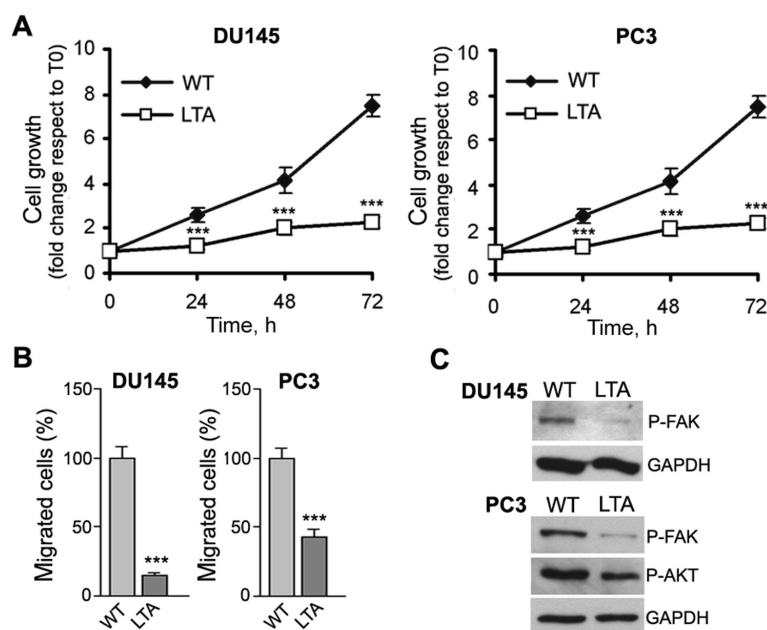
Figure 4. Biological and molecular properties of XN-adapted DU145 and PC3 cells. Cells adapted to long-term exposure to 10 µmol/L XN (DU145-LTA, PC3-LTA) and maintained in the presence of the drug show reduced proliferation rate (A; ***$P < 0.001$) and reduced migration (B; ***$P < 0.001$) when compared with parental cells (WT) grown in the absence of XN. These events correlate with a lower basal phosphorylation status of both FAK and AKT in LTA cells compared with WT cells (C). T0, time zero.

migration hindrance takes place early and in the absence of cell growth arrest (data not shown and Figure 1A).

XN Impairs Molecular Mediators Involved in PCa Cell Proliferation, Migration and Invasive Capacity

FAK is a nonreceptor tyrosine kinase that plays an important role in signal transduction and is a key regulator of survival, proliferation, migration and invasion. Overexpression and/or increased activity of FAK is common in a wide variety of human cancers, implicating a role for FAK in carcinogenesis. DU145 and PC3 cells express high levels of activated FAK, which was rapidly (5 h) downregulated by XN (Figure 3A). Because FAK activation correlates with increased VEGF levels and prostate tumor angiogenesis (23), we determined VEGF release in XN-treated cells by ELISA. Indeed, XN-induced FAK downregulation was associated with reduced VEGF secretion (Figure 3B), confirming

our previously reported data on the antiangiogenic potential of XN (11). FAK signaling can operate via activation of the PI3K/AKT pathway (24) that in turn promotes PCa cell survival, migration and invasion (25).

The AKT activator IGF-I is a potent mitogenic and motogenic factor and has a role in protection against apoptosis and cell survival; it has also been implicated in the initiation and progression of PCa (26). Activation of AKT signaling by a short exposure to IGF-I (30 min at 100 ng/mL) was lowered by XN pretreatment (Figure 3C). IGF-I also significantly stimulated DU145 and PC3 migration, and coexposure to XN completely abrogated the effect (Figure 3D). These molecular events may have a relevant role in mediating both the cytostatic effect and the migratory ability in XN-treated PCa cells.

Downstream of FAK and AKT, the constitutive activation of the NF-κB nuclear transcription factor was found to play an important role in cell prolifera-

tion and cancer development (27,28). We tested whether in PCa cells the biological activities of XN are also mediated through NF-κB modulation, as we reported for endothelial cells (11) and myeloid leukemias (15,16). To investigate the effects of XN on NF-κB, we used TNF-α exposure as a positive activator. ELISA analysis showed that pretreatment with XN for 5 h significantly reduced TNF-α–induced NF-κB activation in a dose-dependent manner (Figure 3E).

We asked whether the observed signaling was related to the sensitivity of cells to XN. We generated DU145 and PC3 cell lines resistant to 10 µmol/L XN by *in vitro* incubation of cells with increasing concentrations of XN; cell lifespan of adapted cells in the presence of 10 µmol/L XN did not exceed 1–2 months, indicating that cells are unable to completely evade XN activity. We thus extended our analyses to adapted clones. Figure 4 shows that in the presence of XN, long-term adapted cultures of DU145 and PC3 cells (DU145-LTA, PC3-LTA) grow (Figure 4A) and migrate (Figure 4B) to a lower extent than parental cells (WT) grown in the absence of XN, and this correlates with decreased basal levels of phosphorylated FAK and AKT (Figure 4C). These data suggest that although cells can become adapted to the drug, the continuous exposure to XN seems to select a less aggressive cell population still responding to XN and not properly defined resistant cells.

ROS Induction Is Involved in the Antitumor Effects of XN

Redox regulation has been shown to play a crucial role in cell survival and modulation of AKT and NF-κB signal transduction pathways (29). We and others already reported that the antitumor effects of XN can be mediated, at least in part, by its capacity to induce ROS overproduction (16,30). In both DU145 and PC3 cells, ROS elevation by 10 µmol/L XN, as detected by the increase of H2-DCFDA fluorescence, was
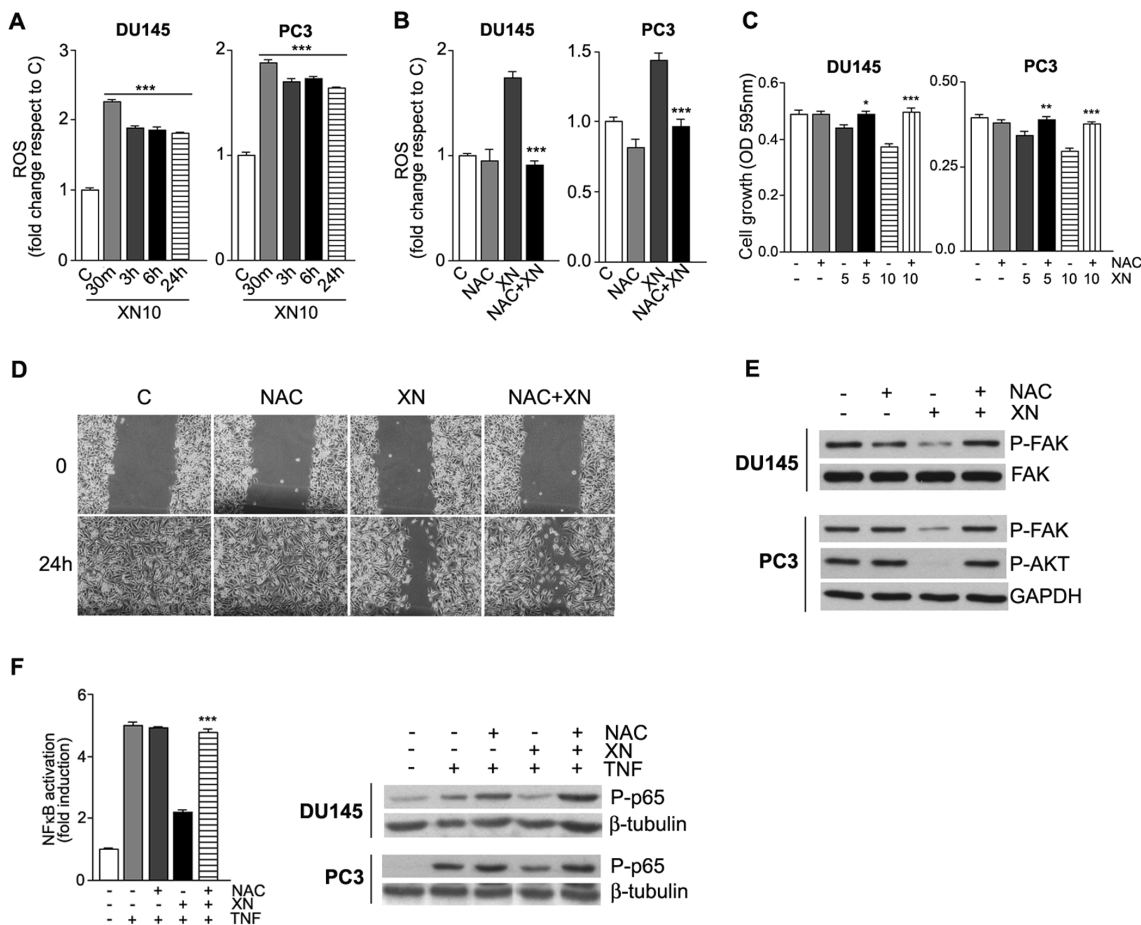
Figure 5. XN induces ROS production in PCa cells. The antioxidant NAC abrogates all the biological effects of XN. Time course of DU145 and PC3 cells treated with 10 μmol/L XN and then stained with H_2DCFDA to assess intracellular ROS levels show a maximal ROS induction after 30 min that is maintained up to 24 h (A). Pretreatment for 90 min with NAC (10 mmol/L) completely inhibited ROS induction by XN (10 μmol/L) at 30 min (B). DU145 and PC3 cell growth inhibition in the presence of 5 and 10 μmol/L XN for 48 h is completely abolished by cotreatment with 10 mmol/L NAC (C). Means ± SD are shown (*$P < 0.05$, **$P < 0.01$, ***$P < 0.001$). PC3 cell migration in the presence of 10 μmol/L XN, evaluated in a 24-h wound healing assay, is restored by 10 mmol/L NAC (D). Western blot analyses of FAK and AKT phosphorylation in DU145 and PC3 cells exposed for 5 h to 10 μmol/L XN in the presence of NAC (alone or in combination) indicates that ROS inhibition restores the basal phosphorylation level of both kinases, even in the presence of XN (E). The ELISA test (PC3 cells are shown) and Western blotting analysis in both cell lines showed that pretreatment with NAC abolished the inhibitory activity of 10 μmol/L XN (5 h treatment) on NF-κB in TNF-α (10 ng/mL) stimulated cells; NAC alone produced marginal effects (F). ELISA data are shown as means ± SD (***$P < 0.001$). Western blot representative results from one of two independent experiments are shown. C (within panels A, B, and D), control; OD, optical density.

an early event, doubling within 30 min of exposure to the drug (Figure 5A) and remaining higher than control cells hereafter. In the presence of the antioxidant NAC (10 mmol/L), ROS induction by XN (10 μmol/L for 30 min) was abrogated in both cell lines (Figure 5B). To explore the possibility that ROS induction by XN takes part to the biological effects described, cell growth and wound-healing assays were carried out

in the presence of NAC at 10 mmol/L. At 48 h, cell growth inhibition by 5 and 10 μmol/L XN was hampered by the presence of NAC in both DU145 and PC3 cells (Figure 5C). At later times (96 h), NAC itself showed inhibitory effects as already described in other cell lines (31) (data not shown). DU145 and PC3 cells were pretreated for 2 h with NAC, and then cell migration in the presence of 10 μmol/L XN was determined by the

wound-healing assay. An increase of cells in the wounded area was observed in NAC-XN–treated cells compared with XN-treated cells (Figure 5D; PC3 cells are shown). We then investigated the effects of XN-induced ROS on the signaling pathways we identified as mediators of the biological effects of XN in PCa cells. Western blot analyses on lysates from cells pretreated with NAC and then exposed to XN for 5 h showed
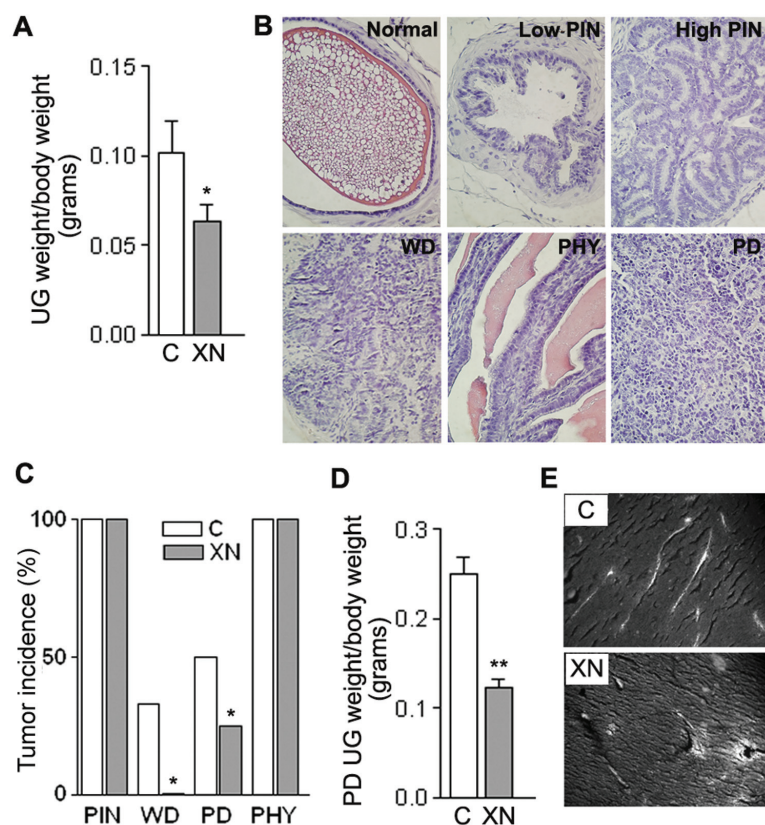
Figure 6. Oral administration of XN in TRAMP mice reduces UG tract weights and retards adenocarcinoma progression. (A) UG weight average of 20 TRAMP mice/group, treated with vehicle alone or XN. Means ± SD are shown (P = 0.046). (B) H&E staining of typical dorsolateral prostate from TRAMP mice: histological grades classified as normal, low- and high-grade PIN, WD carcinoma, PHY and PD carcinoma (40× magnification). (C) Representative fields of each section of each mouse (10 animals/group) were scored for incidence of each histological grade: all animals (control and XN-treated) presented PIN (low and high PINs were classified together) and PHY lesions (100% incidence), whereas WD and PD carcinoma incidence decreased in XN-fed mice (*P < 0.05). (D) The UG weight average from PD-bearing animals, normalized to total body weight, was significantly lower in XN-treated mice (P = 0.003), indicating a strongly reduced PD tumor growth in treated animals. (E) Vessel analyses from 10-μm-thick tissue slices of PD samples show a mature vasculature covering large areas of the tumor in control samples; this structure is partially lost in XN-treated mice where vessels with extravascular erythrocytes are evident (20× magnification). C (within panels A and E), control.

XN Administration Does Not Prevent the Initiation of Carcinogenesis but Retards the Progression of Prostate Adenocarcinoma in TRAMP Mice

TRAMP mice develop spontaneous multistage prostate carcinogenesis that exhibits both histological and molecular features recapitulating many salient aspects of human PCa (33,34). Accordingly, the TRAMP model has been used to successfully test the chemopreventive efficacy of several natural anticancer agents (35–39).

Mice treated by oral gavage with XN three times a week did not exhibit any symptoms of toxicity, and no effects were observed in the body weight profiles when XN-treated mice were compared with vehicle-fed controls (data not shown). At the time of necropsy, all animals were examined for gross pathology, and there was no evidence of edema or abnormal organ size in target and non-target organs. However, there was a significant difference in UG tract weight between control (3.217 ± 0.5503 g) and the XN-fed group (1.892 ± 0.2814 g). When UG tract weight was normalized to body weight (Figure 6A), XN-fed mice showed 40% (P = 0.046) lower UG tract weight than controls. H&E-stained sections (Figure 6B) were microscopically examined and classified on the basis of Kaplan-Lefko *et al.* (20) as normal, PIN (low, high), WD (well differentiated), MD (moderately differentiated), PD (poorly differentiated) and PHY lesions. Histopathologic analysis revealed (a) the absence of MD tumors in both groups, (b) the presence of PIN (low, high) and PHY lesions in all the samples (100% incidence), (c) the presence of WD tumors in the control group only (three out of ten samples) and (d) a doubled PD incidence in the control group (Figure 6C).

The incidence of PIN lesions was found almost identical in both groups, suggesting that XN is unable to exert an inhibitory activity against tumor initiation in the TRAMP model (low and high PINs were clustered together, not showing differences as separated categories). When we looked at PD tumors, their av-

that XN-induced ROS elevation controls the phosphorylation status of FAK and AKT (Figure 5E). Activation of the NF-κB pathway is under ROS-mediated control in some cell systems (32); above a certain threshold, ROS may negatively affect this signaling through interference with the DNA-binding activity of nuclear NF-κB, which requires a reduced conformation. This ROS-mediated mechanism could contribute to the lower NF-κB–binding activity we observed in cells exposed to XN and stimulated with TNF-α (Figure 3E). The ELISA test and Western blotting analyses (Figure 5F) confirmed that NAC strongly and significantly ameliorated NF-κB–binding activity in TNF-α–stimulated cells in the presence of XN. Taken together, these data suggest that induction of ROS participates in the mechanisms of action of XN.

erage weight decreased by 51% in the treated group, and the difference increased to 57.3% when normalized to body weight (Figure 6D, *P* = 0.03). PD tumors appeared highly vascularized; since we previously reported the antiangiogenic properties of XN in highly vascularized Kaposi's sarcoma tumor (11), we analyzed the vascular network in control and XN-treated PD tumors. As shown in Figure 6E and Supplementary Figure S2, the vascular network covered large areas of the tumor; the vascular structure was altered in XN-treated mice where we noticed recurrent vessels with extravascular erythrocytes, indicative of XN effects on the integrity of the vascular walls. Because the endothelium is quite sensitive to the dose of VEGF to which it is exposed, the strong reduction in VEGF production observed (see Figure 3B) after XN exposure may well explain the vascular disruption we observed. Vascularization appeared normal and vessel structure remained unaltered in PIN lesions and in nontumor areas of the prostate of treated animals (data not shown).

DISCUSSION

The main findings of the present study are the evidence that XN blocks cell growth, cell motility and invasive capacity in human PCa cells, irrespective of their p53 and PTEN status, by ROS-mediated targeting of FAK/AKT/NF-κB signaling, and that XN reduces the growth of PD prostate tumors in TRAMP mice without adverse side effects.

Accumulating evidence suggests that constitutive activation of the AKT signaling due to PTEN disabling or other causes is one of the mechanisms involved in the progression of PCa (40). A role for age-dependent AKT activation and increased proliferation of transformed cells in TRAMP PCa progression has been reported (41), and this trend in AKT activation achieved significance by 18 wks of age. Our previous studies also reported highly phosphorylated AKT in PD specimens from 24-wk-old TRAMP mice (42). Activation of the AKT path-

way confers a survival/growth advantage to cancer cells via the positive regulation of NF-κB, increased invasiveness and interference with apoptosis. *In vitro*, we observed decreased AKT and FAK phosphorylation and a reduction of NF-κB activity by short exposure to XN, which *in vivo* may specifically inhibit the proliferation of advanced PD tumors. On the other hand, constitutive low levels of phosphorylated FAK and AKT in cells adapted to long-term XN exposure, as compared with parental cancer cells, suggests that XN may lead to the selection of a less aggressive tumor cell phenotype. These observations suggest that XN might be suitable for long-lasting secondary chemoprevention of advanced cancer after prostatectomy.

Metastasis is the major cause of death in PCa patients (43). The pathogenesis of metastasis is dynamic and complex, involving a series of molecular events including synthesis and secretion of several angiogenic factors to promote neovascularization, motility and local invasion of the host stroma. Wound-healing analysis and *in vitro* migration and invasion assays showed that XN treatment inhibited both cell motility and invasive capacity. Reduced activation of the FAK-mediated motility of PCa cells (44,45) and reduced VEGF secretion together with the antiangiogenic properties of XN (11) highlights additional pathways for its anticancer activity. The identification of FAK, AKT and NF-κB as key molecules involved in the process of carcinogenesis has opened perspectives for devising new therapies (46).

The AKT and NF-κB survival signaling cascades are influenced by the intracellular redox state and tightly balanced by the cellular antioxidant systems (29). In the present study, we report rapid ROS induction by XN. Importantly, the biological effects and molecular modifications induced by XN were prevented by pre- or cotreatment with the antioxidant NAC, indicating that ROS induction is a trigger for the observed effects. As demonstrated by Strathmann *et al.* (30), the effective XN concentration for half-

maximal anion superoxide (O_2^-) induction was significantly higher in the benign prostatic hyperplasia cell line BPH-1 than in the malignant PCa cell line PC3, indicating that increasing malignancy of PCa cells may confer more sensitivity to XN-mediated O_2^- formation, in accordance to our *in vivo* model where XN exerted its inhibitory activity on advanced tumors. Recent studies demonstrated selective killing of cancer cells by polyphenols via ROS-mediated mechanisms both *in vitro* and *in vivo* (47). This result implicates preventive and therapeutic benefits by dietary supplementation with polyphenols. An initial safety study in rats (48) revealed no toxic side effects of XN when administered at 100 mg/kg body weight per day for extended periods of time. Peak plasma concentrations after a single application of 1,000 mg/kg body weight to female rats were detected after 4 h, reaching 3.1 μmol/L (49).

In vivo, under the regimen we have tested in TRAMP mice, XN caused an evident decrease in UG tract weight and affected the incidence of WD and PD adenocarcinomas, but did not reduce the mean incidence of PIN lesions and PHY structures. The equivalent occurrence of PINs could be predictable, since early epithelial transformation of prostatic cells is driven, in TRAMP mice, by SV40 large T antigen expressed under the probasin promoter in all prostate epithelial cells and not by spontaneous/random mutations that could be scavenged by XN. This observation is sustained by the lack of inflammatory reactions in TRAMP PIN lesions, whereas this is a typical feature of human PINs. The same viral antigen-driven origin could also be applicable to the stromal PHY lesions, for which origin and biology remains controversial also in humans.

A significant effect of XN was observed on the incidence of advanced tumors. Although rare, WD tumors were found only in control mice, whereas the number of PD tumors was halved in XN-treated animals. XN was also able to reduce PD tumor size, indicating that the advanced

stages of TRAMP carcinogenesis, linked to the activity of additional mutational and promoting effectors, are affected by XN activity. These remarkable effects are in line with those observed *in vitro* in advanced human PCa cell lines. Reduced secretion of angiogenic factors, including VEGF (see Figure 3B), in the tumor microenvironment by PCa after XN exposure, along with the antiangiogenic effects of FAK inhibition (50), might in part explain the presence of abnormal vessels and hemorrhage in PD tumors. Emerging data from early-phase clinical trials with orally available small-molecule inhibitors of FAK are promising. In the future, combination therapy with cytotoxic or antiangiogenic drugs may help to overcome chemoresistance and enhance efficacy of antivascular therapy.

In humans, PCa progresses slowly through well-defined stages characterized by initial hyperplasia and subsequent development of adenocarcinoma, allowing a window of opportunity to either stop or delay the progression of the disease. Although the incidence of latent, noninfiltrative prostate carcinomas is similar in Asian and Western populations, clinically relevant carcinomas and PCa mortality are higher in Western countries (51). This observation prompted several studies aimed at determining the chemopreventive effects of molecules targeting different signaling pathways involved in tumor progression (17,35,41,52).

CONCLUSION

Here, we have shown that XN, at the low-dose schedule tested achievable in the clinic, affects PCa cell growth *in vitro* and reduces progression and growth of advanced tumors in TRAMP mice without any adverse health effect. Potential mechanisms of this anti-PCa effect of XN are most likely due to the down-modulation of FAK/AKT/NF-κB signaling by ROS, leading to the inhibition of cell cycle progression accompanied by decreased cell migration and invasion and possibly a secondary selection of less aggressive cellular clones.

Taken together, these data suggest that XN could be a suitable cancer preventive agent in chemoprevention of advanced PCa to contrast progression and to delay relapse of surgically treated patients.

DISCLOSURE

The authors declare that they have no competing interests as defined by *Molecular Medicine*, or other interests that might be perceived to influence the results and discussion reported in this paper.

REFERENCES

1. Jemal A, *et al.* (2007) Cancer statistics, 2007. *CA Cancer J. Clin*. 57:43–66.
2. Debruyne F. (2002) Hormonal therapy of prostate cancer. *Seminars in Urologic Oncology*. 20:4–9.
3. Liang J, Slingerland JM. (2003) Multiple roles of the PI3K/PKB (Akt) pathway in cell cycle progression. *Cell Cycle*. 2:339–45.
4. Bertram J, *et al.* (2006) Loss of PTEN is associated with progression to androgen independence. *Prostate*. 66:895–902.
5. Corson TW, Crews CM. (2007) Molecular understanding and modern application of traditional medicines: triumphs and trials. *Cell*. 130:769–74.
6. Gerhauser C, *et al.* (2002) Cancer chemopreventive activity of Xanthohumol, a natural product derived from hop. *Mol. Cancer Ther*. 1:959–69.
7. Lust S, *et al.* (2005) Xanthohumol kills B-chronic lymphocytic leukemia cells by an apoptotic mechanism. *Mol. Nutr. Food Res*. 49:844–50.
8. Vanhoecke B, *et al.* (2005) Antiinvasive effect of xanthohumol, a prenylated chalcone present in hops (Humulus lupulus L.) and beer. *Int. J. Cancer*. 117:889–95.
9. Pan L, Becker H, Gerhauser C. (2005) Xanthohumol induces apoptosis in cultured 40–16 human colon cancer cells by activation of the death receptor- and mitochondrial pathway. *Mol. Nutr. Food Res*. 49:837–43.
10. Delmulle L, Vanden Berghe T, Keukeleire DD, Vandenabeele P. (2008) Treatment of PC-3 and DU145 prostate cancer cells by prenylflavonoids from hop (Humulus lupulus L.) induces a caspase-independent form of cell death. *Phytother. Res*. 22:197–203.
11. Albini A, *et al.* (2006) Mechanisms of the antiangiogenic activity by the hop flavonoid xanthohumol: NF-kappaB and Akt as targets. *FASEB J*. 20:527–9.
12. Colgate EC, Miranda CL, Stevens JF, Bray TM, Ho E. (2007) Xanthohumol, a prenylflavonoid derived from hops induces apoptosis and inhibits NF-kappaB activation in prostate epithelial cells. *Cancer Lett*. 246:201–9.
13. Lee SH, Kim HJ, Lee JS, Lee IS, Kang BY. (2007) Inhibition of topoisomerase I activity and efflux drug transporters' expression by xanthohumol from hops. *Arch. Pharm. Res*. 30:1435–9.
14. Zhao F, Nozawa H, Daikonnya A, Kondo K, Kitanaka S. (2003) Inhibitors of nitric oxide production from hops (Humulus lupulus L.). *Biol. Pharm. Bull*. 26:61–5.
15. Dell'Eva R, *et al.* (2007) AKT/NF-kappaB inhibitor xanthohumol targets cell growth and angiogenesis in hematologic malignancies. *Cancer*. 110:2007–11.
16. Monteghirfo S, *et al.* (2008) Antileukemia effects of xanthohumol in Bcr/Abl-transformed cells involve nuclear factor-kappaB and p53 modulation. *Mol. Cancer Ther*. 7:2692–702.
17. Benelli R, Monteghirfo S, Vene R, Tosetti F, Ferrari N. (2010) The chemopreventive retinoid 4HPR impairs prostate cancer cell migration and invasion by interfering with FAK/AKT/GSK3beta pathway and beta-catenin stability. *Mol. Cancer*. 9:142.
18. Committee for the Update of the Guide for the Care and Use of Laboratory Animals, Institute for Laboratory Animal Research, Division on Earth and Life Studies, National Research Council of the National Academies. (2011) *Guide for the Care and Use of Laboratory Animals*. 8th edition. Washington (DC): National Academies Press. [cited 2011 Sep 1]. Available from: http://oacu.od.nih.gov/regs/
19. Greenberg NM, *et al.* (1995) Prostate cancer in a transgenic mouse. *Proc. Natl. Acad. Sci. U. S. A*. 92:3439–43.
20. Kaplan-Lefko PJ, *et al.* (2003) Pathobiology of autochthonous prostate cancer in a pre-clinical transgenic mouse model. *Prostate*. 55:219–37.
21. Larghero P, *et al.* (2007) Biological assays and genomic analysis reveal lipoic acid modulation of endothelial cell behavior and gene expression. *Carcinogenesis*. 28:1008–20.
22. Deeb D, *et al.* (2010) Growth inhibitory and apoptosis-inducing effects of xanthohumol, a prenylated chalone present in hops, in human prostate cancer cells. *Anticancer Res*. 30:3333–9.
23. Pang X, *et al.* (2011) 1′-Acetoxychavicol acetate suppresses angiogenesis-mediated human prostate tumor growth by targeting VEGF-mediated Src-FAK-Rho GTPase-signaling pathway. *Carcinogenesis*. 32:904–12.
24. Sonoda Y, Watanabe S, Matsumoto Y, Aizu-Yokota E, Kasahara T. (1999) FAK is the upstream signal protein of the phosphatidylinositol 3-kinase-Akt survival pathway in hydrogen peroxide-induced apoptosis of a human glioblastoma cell line. *J. Biol. Chem*. 274:10566–70.
25. Shukla S, *et al.* (2007) Activation of PI3K-Akt signaling pathway promotes prostate cancer cell invasion. *Int. J. Cancer*. 121:1424–32.

26. Sachdev D, Yee D. (2007) Disrupting insulin-like growth factor signaling as a potential cancer therapy. *Mol. Cancer Ther*. 6:1–12.

27. Amit S, Ben-Neriah Y. (2003) NF-kappaB activation in cancer: a challenge for ubiquitination- and proteasome-based therapeutic approach. *Semin. Cancer Biol*. 13:15–28.

28. Aggarwal BB. (2004) Nuclear factor-kappaB: the enemy within. *Cancer Cell*. 6:203–8.

29. Lau AT, Wang Y, Chiu JF. (2008) Reactive oxygen species: current knowledge and applications in cancer research and therapeutic. *J. Cell. Biochem.* 104:657–67.

30. Strathmann J, *et al.* (2010) Xanthohumol-induced transient superoxide anion radical formation triggers cancer cells into apoptosis via a mitochondria-mediated mechanism. *FASEB J*. 24:2938–50.

31. Albini A, *et al.* (2001) Inhibition of angiogenesis-driven Kaposi's sarcoma tumor growth in nude mice by oral N-acetylcysteine. *Cancer Res.* 61:8171–8.

32. Bubici C, Papa S, Dean K, Franzoso G. (2006) Mutual cross-talk between reactive oxygen species and nuclear factor-kappa B: molecular basis and biological significance. *Oncogene*. 25:6731–48.

33. Gingrich JR, *et al.* (1997) Androgen-independent prostate cancer progression in the TRAMP model. *Cancer Res.* 57:4687–91.

34. Klein RD, Kant JA. (2006) Opportunity knocks: the pathologist as laboratory genetics consultant. *Arch. Pathol. Lab. Med.* 130:1603–4.

35. Gupta S, Hastak K, Ahmad N, Lewin JS, Mukhtar H. (2001) Inhibition of prostate carcinogenesis in TRAMP mice by oral infusion of green tea polyphenols. *Proc. Natl. Acad. Sci. U. S. A.* 98:10350–5.

36. Raina K, Singh RP, Agarwal R, Agarwal C. (2007) Oral grape seed extract inhibits prostate tumor growth and progression in TRAMP mice. *Cancer Res.* 67:5976–82.

37. Singh SV, *et al.* (2009) Sulforaphane inhibits prostate carcinogenesis and pulmonary metastasis in TRAMP mice in association with increased cytotoxicity of natural killer cells. *Cancer Res.* 69:2117–25.

38. Pannellini T, *et al.* (2010) A dietary tomato supplement prevents prostate cancer in TRAMP mice. *Cancer Prev Res (Phila).* 3:1284–91.

39. Singh SV, *et al.* (2008) Garlic constituent diallyl trisulfide prevents development of poorly differentiated prostate cancer and pulmonary metastasis multiplicity in TRAMP mice. *Cancer Res.* 68:9503–11.

40. Li L, *et al.* (2005) The emerging role of the PI3-K-Akt pathway in prostate cancer progression. *Prostate Cancer Prostatic Dis*. 8:108–18.

41. El Touny LH, Banerjee PP. (2007) Akt GSK-3 pathway as a target in genistein-induced inhibition of TRAMP prostate cancer progression toward a poorly differentiated phenotype. *Carcinogenesis*. 28:1710–7.

42. Ciarlo M, *et al.* (2012) Regulation of neuroen-docrine differentiation by AKT/hnRNPK/AR/beta-catenin signaling in prostate cancer cells. *Int. J. Cancer*. 131:582–90.

43. Nelson WG, De Marzo AM, Isaacs WB. (2003) Prostate cancer. *N Engl. J. Med.* 349:366–81.

44. Senapati S, *et al.* (2010) Overexpression of macrophage inhibitory cytokine-1 induces metastasis of human prostate cancer cells through the FAK-RhoA signaling pathway. *Oncogene*. 29:1293–302.

45. Slack JK, *et al.* (2001) Alterations in the focal adhesion kinase/Src signal transduction pathway correlate with increased migratory capacity of prostate carcinoma cells. *Oncogene*. 20:1152–63.

46. Schmidmaier R, Baumann P. (2008) ANTI-ADHESION evolves to a promising therapeutic concept in oncology. *Curr. Med. Chem*. 15:978–90.

47. Trachootham D, *et al.* (2006) Selective killing of oncogenically transformed cells through a ROS-mediated mechanism by beta-phenylethyl isothiocyanate. *Cancer Cell*. 10:241–52.

48. Hussong R, *et al.* (2005) A safety study of oral xanthohumol administration and its influence on fertility in Sprague Dawley rats. *Mol. Nutr. Food Res*. 49:861–7.

49. Gerhauser C. (2005) Beer constituents as potential cancer chemopreventive agents. *Eur. J. Cancer*. 41:1941–54.

50. Lechertier T, Hodivala-Dilke K. (2012) Focal adhesion kinase and tumour angiogenesis. *J. Pathol.* 226:404–12.

51. Yatani R, *et al.* (1982) Geographic pathology of latent prostatic carcinoma. *Int. J. Cancer*. 29:611–6.

52. Shukla S, *et al.* (2007) Blockade of beta-catenin signaling by plant flavonoid apigenin suppresses prostate carcinogenesis in TRAMP mice. *Cancer Res.* 67:6925–35.